

PAPER • OPEN ACCESS

Analysis of two-dimensional (2D) Fruit Drying Process through Heat and Mass Transfer Model

To cite this article: N Shahari *et al* 2019 *IOP Conf. Ser.: Mater. Sci. Eng.* **477** 012024

View the [article online](#) for updates and enhancements.

Analysis of two-dimensional (2D) Fruit Drying Process through Heat and Mass Transfer Model

N Shahari , H A Hasnan , A Y Hanan and N A H Noor Ishak

Faculty of Computer and Science Mathematics, Universiti Teknologi MARA,
Seremban, Negeri Sembilan, Malaysia

E-mail: norazni@ns.uitm.edu.my

Abstract. The production of dried fruit occurs when there is removal of water content, either naturally, through sun drying, or through the use of the specialized dryers. However, the amount of water left and the temperature inside the fruit cannot be accurately known and only a rough idea is obtained by observation during the drying process. In this paper, two-dimensional fruit drying was analysed through Fick's Law of Diffusion and Fourier's Law of Heat Conduction to allow the effect on the front and rear faces of the fruit to be shown during drying. These equations were used and solved using the Finite-Difference Method (FDM). The result shows that, as time increases, the moisture content decreases and this occurs at each location of the fruit. The reduction rate of moisture in the region near the surface is higher than the interior of the fruit because of the high initial moisture gradient in this region, which drives diffusion from the inside to the surface. The model allows us to predict temperature and moisture distribution as time increases. A Graphical User Interface (GUI) was developed, which can present the results graphically and can aid the development of a food product. The model will be presented in such a way that it can be used by those less familiar with the process of drying, and so that it can be adapted for different food products.

1. Introduction

One of the benefits of the drying process is to prevent the growth of bacteria, yeast and mould. In general, drying is the removal of water content and involves two phases: the initial phase is called the constant-rate drying period while the second phase is called the falling-rate drying period. The drying rate is constant during the initial phase when the water inside the fruit will be transferred to the surface. Once the fruit has dried sufficiently, the falling-rate drying period begins and the drying rate continuously decreases. Thus, drying can be described as the reduction of fruit moisture to the necessary dryness values as a specific process [1]. Necessary dryness value is important since it is one of the aspects of product quality. Furthermore, drying can also be considered as the process whereby heat and mass transfer occurs simultaneously [2].

During drying, heat is gained by convection when the outer surface is warmed up by the surrounding air. From this, the heat transfer coefficients exist at the surface of the fruit. Then, the inner part of the fruit will warm up towards the region that is in contact with the outer surface as the heat is transferred from a hotter region to a colder region by conduction. Generally, diffusion is the movement of water from a higher concentration to a lower concentration. In the drying process, the water diffuses out from the inner part of the fruit to the surface. Then, heat changes the water to water vapour at the surface. It causes the moisture inside the fruit to reduce. Thus, a mass transfer coefficient exists at the surface.



The most common modelling in food involves a one-dimensional model (1D), in which food can be assumed to be of infinite length with moisture and temperature given across the thickness of the food. This method has been used to analyse drying behaviour [3-6]. For the drying of slices of food with the cross-sectional area of a rectangle, a two-dimensional model (2D) is used to allow the effect of geometry to be included. Some researchers have investigated the two-dimensional model [2], [7-9]. The various models proposed for convective drying of a food product using heat and mass transfer (1D, 2D or 3D) can be found in [6]. Various theoretical models proposed in the literature for the drying of foods linked the heat equation with the mass equation by using the latent heat evaporation boundary condition at the surface in the heat equation. However, the driving gradient from the surface to the air that involves partial pressure and temperature at the surface of the mass equation was not considered. In this research, the analysis focused on two dimensional fruit with the application of coupled boundary conditions, both for mass and heat equations ([10]).

2. Methodology

2.1. Mathematical model

The diffusion and heat equation is applied to describe the two-dimensional movement of moisture (M) and temperature (T) in fruits. In the Cartesian coordinates with mass diffusivity of fruit, D (m^2/s) and thermal diffusivity of heat, α (m^2/s), the general equation for moisture and temperature at any time, t (s) is given by:

$$\frac{\partial M(x, y, t)}{\partial t} = D \left(\frac{\partial^2 M}{\partial x^2} + \frac{\partial^2 M}{\partial y^2} \right), \quad 0 < x < L_x, \quad 0 < y < L_y, \quad (1)$$

$$\frac{\partial T(x, y, t)}{\partial t} = \alpha \left(\frac{\partial^2 T}{\partial x^2} + \frac{\partial^2 T}{\partial y^2} \right), \quad 0 < x < L_x, \quad 0 < y < L_y, \quad (2)$$

where x and y represent the thickness and length of the fruit (mm).

The boundary conditions are given below:

$$x = 0, \quad \frac{\partial M(0, y, t)}{\partial x} = 0, \quad \frac{\partial T(0, y, t)}{\partial x} = 0, \quad (3)$$

$$y = 0, \quad \frac{\partial M(x, 0, t)}{\partial y} = 0, \quad \frac{\partial T(x, 0, t)}{\partial y} = 0 \quad (4)$$

$$x = L_x, \quad -D \frac{\partial M(L_x, y, t)}{\partial x} = h_m (C_{sur} - C_{air}), \quad (5)$$

$$-h(T_{sur} - T_{air}) = k \frac{\partial T(L_x, y, t)}{\partial x} - \lambda D \rho_s \frac{\partial M(L_x, y, t)}{\partial x},$$

$$y = L_y, \quad -D \frac{\partial M(x, L_y, t)}{\partial y} = h_m (C_{sur} - C_{air}), \quad (6)$$

$$-h(T_{sur} - T_{air}) = k \frac{\partial T(x, L_y, t)}{\partial y} - \lambda D \rho_s \frac{\partial M(x, L_y, t)}{\partial y}.$$

The initial condition is as follows:

$$t = 0, \quad M(x, y, 0) = M_0, T(x, y, 0) = T_0. \quad (7)$$

2.2. Non-Dimension

In order to solve and produce an equation with scale $0 < \bar{x} < 1$, and scale of $0 < \bar{y} < 1$, the equation is then dimensionalized in a non-dimensional formulation. The non-dimensional scaled variables used are representative of diffusion timescale, τ ; scaled moisture content, \bar{M} ; and scaled temperature, \bar{T} .

$$\tau = \frac{Dt}{L_x^2}, \quad \bar{M} = \frac{M}{M_0}, \quad \bar{T} = \frac{T - T_0}{T_{air} - T_0}, \quad \bar{x} = \frac{x}{L_x}, \quad \bar{y} = \frac{y}{L_y}.$$

By applying the dimensional scaled variables, the non-dimensional variables of moisture and temperature equations, ((1)-(7)) are simplified and arranged as follows:

$$\frac{\partial \bar{M}(\bar{x}, \bar{y}, \tau)}{\partial \tau} = \frac{\partial^2 \bar{M}}{\partial \bar{x}^2} + \beta^2 \frac{\partial^2 \bar{M}}{\partial \bar{y}^2}, \quad \text{where } \beta = \frac{L_x}{L_y}, \quad (8)$$

$$\frac{\partial \bar{T}(\bar{x}, \bar{y}, \tau)}{\partial \tau} = Le \left(\frac{\partial^2 \bar{T}}{\partial \bar{x}^2} + \beta^2 \frac{\partial^2 \bar{T}}{\partial \bar{y}^2} \right). \quad (9)$$

With the boundary equations,

$$\frac{\partial \bar{M}(0, \bar{y}, \tau)}{\partial \bar{x}} = 0, \quad \frac{\partial \bar{T}(0, \bar{y}, \tau)}{\partial \bar{x}} = 0, \quad \frac{\partial \bar{M}(\bar{x}, 0, \tau)}{\partial \bar{y}} = 0, \quad \frac{\partial \bar{T}(\bar{x}, 0, \tau)}{\partial \bar{y}} = 0, \quad (10)$$

$$\frac{\partial \bar{M}(1, \bar{y}, \tau)}{\partial \bar{x}} = -Bi_m \frac{C_{air}}{M_0} (\bar{C}_{sur} - 1), \quad (11)$$

$$\frac{\partial \bar{T}(1, \bar{y}, \tau)}{\partial \bar{x}} = Bi(1 - \bar{T}_{sur}) + \bar{\lambda} \frac{\partial \bar{M}(1, \bar{y}, \tau)}{\partial \bar{x}}, \quad (12)$$

$$\frac{\partial \bar{M}(\bar{x}, 1, \tau)}{\partial \bar{y}} = -\frac{1}{\beta} Bi_m \frac{C_{air}}{M_0} (\bar{C}_{sur} - 1), \quad (13)$$

$$\frac{\partial \bar{T}(\bar{x}, 1, \tau)}{\partial \bar{y}} = \frac{1}{\beta} Bi(1 - \bar{T}_{sur}) + \bar{\lambda} \frac{\partial \bar{M}(\bar{x}, 1, \tau)}{\partial \bar{y}}. \quad (14)$$

And the initial conditions are

$$\bar{M} = 1, \quad \bar{T} = 0. \quad (15)$$

$$\text{where } Bi_m = \frac{h_m L_x}{D}, \quad Bi = \frac{h L_x}{k}, \quad Le = \frac{\alpha}{D}, \quad \bar{\lambda} = \frac{\lambda D \rho_s}{k} \frac{M_0}{(T_{air} - T_0)}, \quad \bar{C}_{sur} = \frac{C_{sur}}{C_{air}}.$$

2.3. Numerical Method

Discretization equations (8) and (9) with a central difference approximation become (the over bar notation is dropped as clarity)

$$T_{i,j}^{n+1} = T_{i,j}^n + sx(T_{i,j+1}^n - 2T_{i,j}^n + T_{i,j-1}^n) + \beta^2 sz(T_{i+1,j}^n - 2T_{i,j}^n + T_{i-1,j}^n), \quad (16)$$

$$M_{i,j}^{n+1} = M_{i,j}^n + mx(M_{i,j+1}^n - 2M_{i,j}^n + M_{i,j-1}^n) + \beta^2 m\zeta(M_{i+1,j}^n - 2M_{i,j}^n + M_{i-1,j}^n), \quad (17)$$

at general index point i and j , for $i=2,3,\dots,Nz-1$ and $j=2,3,\dots,Nx-1$.

$$\text{with } sx = Le * \frac{\Delta t}{\Delta x^2} \text{ and } sz = Le * \frac{\Delta t}{\Delta y^2}, \quad mx = \frac{\Delta t}{\Delta x^2} \text{ and } m\zeta = \frac{\Delta t}{\Delta y^2}.$$

To apply the symmetry condition, a fictitious grid point is involved and the equation is eliminated using central difference approximation. This gives the condition,

$$T_{i,1}^{n+1} = T_{i,1}^n + sx(2T_{i,2}^n - 2T_{i,1}^n) + \beta^2 sz(T_{i+1,1}^n - 2T_{i,1}^n + T_{i-1,1}^n), \quad i = 2, 3, \dots, Nz - 1. \quad (18)$$

$$T_{1,j}^{n+1} = T_{1,j}^n + sx(T_{1,j-1}^n - 2T_{1,j}^n + T_{1,j+1}^n) + \beta^2 sz(2T_{2,j}^n - 2T_{1,j}^n), \quad j = 2, 3, \dots, Nx - 1. \quad (19)$$

$$M_{i,1}^{n+1} = M_{i,1}^n + mx(2M_{i,2}^n - 2M_{i,1}^n) + \beta^2 mz(M_{i+1,1}^n - 2M_{i,1}^n + M_{i-1,1}^n), \quad i = 2, 3, \dots, Nz - 1, \quad (20)$$

$$M_{1,j}^{n+1} = M_{1,j}^n + mx(M_{1,j-1}^n - 2M_{1,j}^n + M_{1,j+1}^n) + \beta^2 mz(2M_{2,j}^n - 2M_{1,j}^n), \quad j = 2, 3, \dots, Nx - 1. \quad (21)$$

Applying the surface condition equation by introducing a fictitious grid point at $x=Nx$ and $y=Nz$ and using central difference approximation gives

$$T_{i,Nx}^{n+1} = T_{i,Nx}^n + sx(2T_{i,Nx-1}^n - 2T_{i,Nx}^n + 2\Delta x Bi (1 - T_{sur})) + \bar{\lambda} * 2\Delta x (3M_{i,Nx}^n - 4M_{i,Nx-1}^n + M_{i,Nx-2}^n) + sz\beta^2 (T_{i+1,Nx}^n - 2T_{i,Nx}^n + T_{i-1,Nx}^n), \quad i = 2, 3, \dots, Nz - 1. \quad (22)$$

$$T_{Nz,j}^{n+1} = T_{Nz,j}^n + sx(T_{Nz,j-1}^n - 2T_{Nz,j}^n + T_{Nz,j+1}^n) + \beta^2 sz\{2T_{Nz-1,j}^n - 2T_{Nz,j}^n + \frac{1}{\beta} [2\Delta z Bi (1 - T_{Nz,j})] + \bar{\lambda} * 2\Delta z (3M_{Nz,j}^n - 4M_{Nz-1,j}^n + M_{Nz-2,j}^n)\}, \quad j = 2, 3, \dots, Nx - 1. \quad (23)$$

$$M_{i,Nx}^{n+1} = M_{i,Nx}^n + mx(2M_{i,Nx-1}^n - 2M_{i,Nx}^n - 2\Delta x Bi_m \frac{C_{air}}{M_0} (C_{sur} - 1)) + mz\beta^2 (M_{i+1,Nx}^n - 2M_{i,Nx}^n + M_{i-1,Nx}^n), \quad i = 2, 3, \dots, Nz - 1. \quad (24)$$

$$M_{Nz,j}^{n+1} = M_{Nz,j}^n + mx(M_{Nz,j-1}^n - 2M_{Nz,j}^n + M_{Nz,j+1}^n) + mz\beta^2 [2M_{Nz-1,j}^n - 2M_{Nz,j}^n - \frac{1}{\beta} 2\Delta z Bi_m \frac{C_{air}}{M_0} (C_{sur} - 1)], \quad j = 2, 3, \dots, Nx - 1. \quad (25)$$

3. Results and Discussions

Solution of the model is obtained by solving two coupled Partial Differential Equations (PDE) corresponding mass and heat equation (equation (8)-(9)), together with initial and boundary conditions (Equation (10)-(14)). Equations (8) and (9) are numerically discretized using the FDM (Equation (16)-(25)) while the derived algebraic equations are solved using MATLAB. For the first simulation, the

thickness and the length are taken as aspect ratio (AR) $\frac{L_x}{L_y} = 1$. The simulation is then repeated with

aspect ratio $\frac{L_x}{L_y} = 2$. The thickness of the food is maintained at constant value $L_x = 1$ and the length

of the food is changed according to the corresponding aspect ratio (AR).

The moisture profile at different time intervals is shown in Figure 1. At the beginning, the moisture drops significantly at the surface of the fruit and there is still much water content inside the fruit. At this time, the fruit is saturated with water at the surface and moisture removal occurs at a faster rate. Once the surface moisture becomes less, moisture from the inside will be transferred by diffusion onto the surface. The process of diffusivity occurs from the inside to the surface of the fruit. As the drying proceeds, the moisture level starts to drop substantially compared to the beginning of the process. The experiment conducted by [11] shows a similar finding: the moisture contents are relatively low towards the surface facing the surrounding air, compared to the inner part of the object. Based on the Figure 1, the longer the time period, the lower the moisture content left inside the fruit.

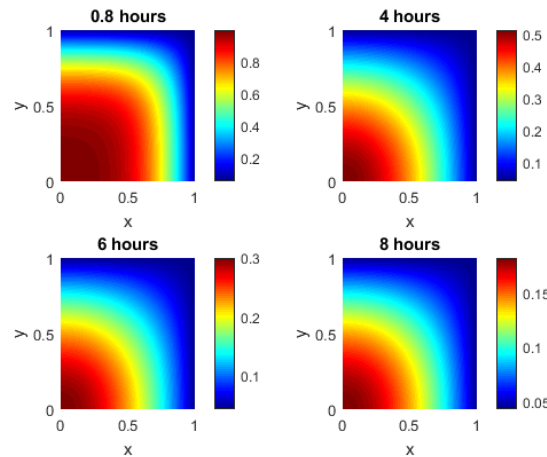


Figure 1. Predicted moisture distribution inside the moist fruit at different time intervals (a) $t = 0.8$ hours, (b) $t = 4$ hours, (c) $t = 6$ hour (d) $t = 8$ hours

Figure 2 shows the distribution of temperature inside the slice at different times. There is a difference between the temperature at the surface and at the core. Initially, the surface temperature starts to increase and the movement of the heat from the surface to the core rises, showing that the temperature inside the fruit has increased. The substantial increase shows that the surface is getting hotter and at the core there is a clear difference between the current temperature inside the fruit and the earlier temperature. This is consistent with findings by [11], which stated that the temperature distributions are higher at the surface of the moist object and these progressively decrease towards the interior portion of the moist object. From these results, the part of the fruit that is most exposed to the surrounding air tends to warm up faster. Thus, the longer the drying period, the higher the temperature at both the surface and the core of the fruit T .

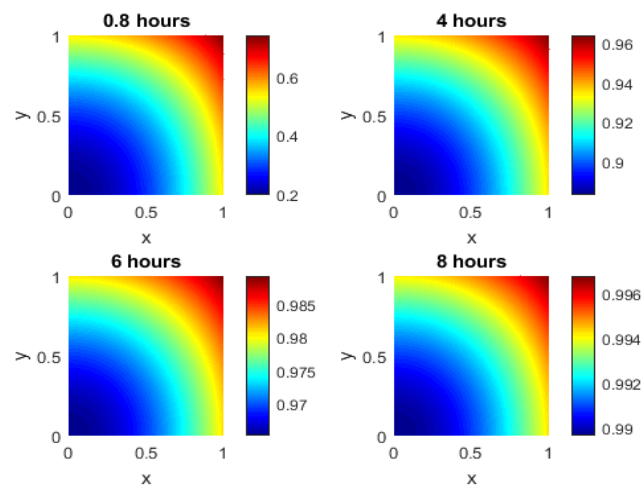


Figure 2. Predicted temperature distribution inside the moist fruit at different time intervals (a) $t = 0.8$ hour, (b) $t = 4$ hour, (c) $t = 6$ hour (d) $t = 8$ hour

Figure 3 clearly shows that the processes of heat and mass transfer occur simultaneously. When the temperature at the surface of fruit rises, the moisture starts to drop sharply near the surface. However, the core of the fruit shows only a small increase in temperature, while the moisture content drops a little. The temperature and moisture stop when equilibrium is achieved. The thin surface region,

having a steep moisture profile, causes a shell to develop on the outside [12]. Normally, heat enters the surface of the fruit by conduction, while water moves outwards from the inside of the fruit by diffusion. At this stage, heat is required to change water to water vapour at the surface of fruit. After that, the water vapour loss to the surrounding area causes the moisture at the surface to decrease. From the result above, the higher the temperature, the lower the moisture level inside the fruit. It indicates that the temperature increases, in contrast to the moisture content.

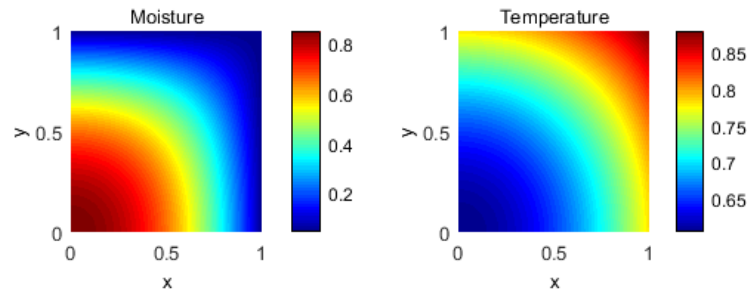


Figure 3. The temperature and moisture distribution after 2 hours when the parameters: $Bi_m=20$, $Bi=1.5$ and $Le=5$

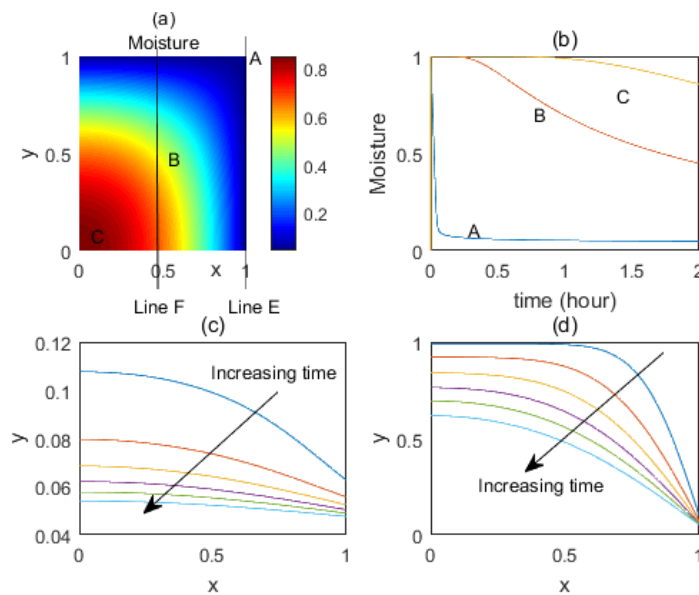


Figure 4. (a) Surface plot of moisture evolution after 2 hours. (b) Moisture decreasing at selected points A, B and C (c) Moisture across a line passing through the surface (line E). (d) Moisture across a line passing through the surface (line F)

Figure 4 and Figure 5 show three characteristic points inside the fruit that were selected: point A-located at the top surface; Point B-located in the middle of the fruit; point C-located in the symmetry point of the fruits. Figure 4(b) shows that the removal of water content at A is higher compared to B and C since point A represents the top surface of the fruit, which is more exposed to the surrounding air. Point C has the lowest water removal because it is located in the middle core of the fruit. Figure 4(c) shows the distribution of moisture at line E, which is located at the outer surface. Figure 4(d) shows the distribution of moisture at line F, which is located in the middle of the surface. From the graph observation, the rate of water removal at line E is higher as time increases, compared to line F.

This is supported by [7] who state that, at the surface, the drying rate is faster than the drying rate inside the fruit since the moisture gradients between the surrounding air and the surface are higher.

Figures 5(a) and 5(b) show that the increase in temperature at A is higher compared to B and C since point A represents the top surface of the fruit, which is more exposed to the surrounding air. Point C has the lowest increase in temperature because it is located in the middle core of the fruit. Figure 5(c) shows the temperature distribution at line E, which is located at the outer surface. Figure 5(d) shows the temperature distribution at line F, which is located in the middle of the surface. From the graph observation, the rate of temperature increase at line E is higher as time increases compared to line F. This finding from [11] states that the heat transfer coefficients, h are higher at the surface because of immediate contact with the hot air.

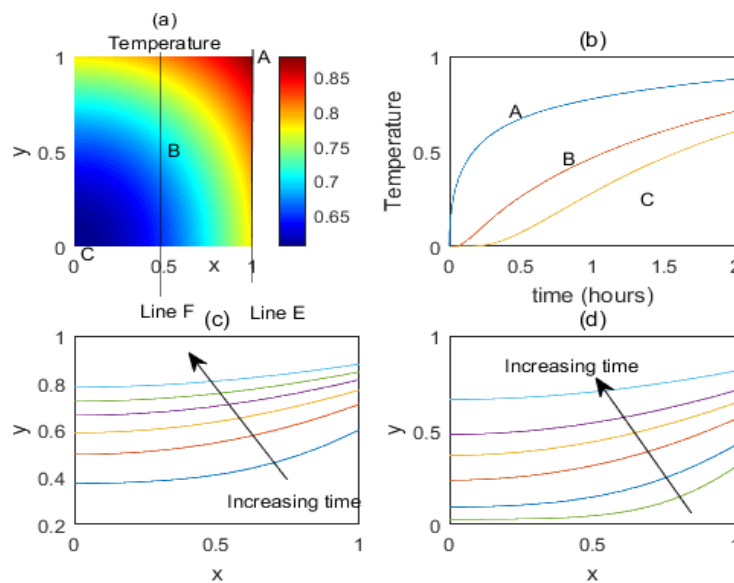


Figure 5. a) Surface plot of temperature evolution at 2.4 hours. b) Temperature is increasing at selected points A, B, and C c) Temperature across a line passing through the surface (line E). d) Temperature across a line passing through the surface (line F)

Variation of moisture inside the fruit with 2 different aspect ratios (AR) is shown in Figure 6. It was observed that moisture reduces more quickly for smaller AR, which concludes that smaller aspect ratios (AR) provide shorter drying times than higher AR. This is consistent with findings by [7], which showed that the drying rate decreases by 4.5% with a 1 mm increase in mango thickness.

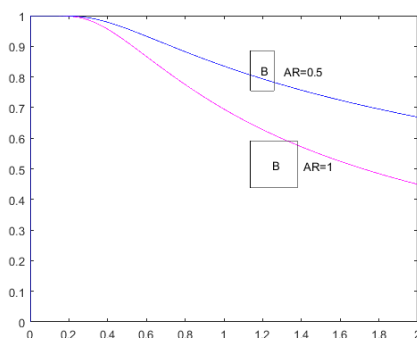


Figure 6. Effect of aspect ratio(AR) on the moisture at a selected points B

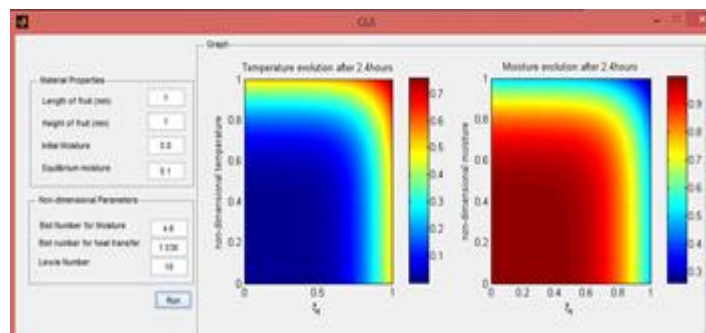


Figure 7. : Graphical User Interface for two-dimensional fruit drying

Figure 7 shows the Graphical User Interface (GUI) that was developed using MATLAB Graphical User Interface Development Environment (GUIDE). The interface was designed to have one major subpanel, material properties and non-dimensional parameters, which compute the material properties of fruit and its non-dimensional parameters. The Graph subpanel has the responsibility of obtaining the results from the GUI core and interpreting the simulation results in human friendly language. After receiving the simulation results, the Graph presents the results of the “Temperature evolution after 2 hours” axes and the “Moisture evolution after 2 hours” axes. The image will be used as a system for monitoring the moisture and temperature inside the fruit.

4. Conclusion

A 2D heat and mass transfer numerical model was developed to study the transient behaviour of temperature and moisture content during the drying of fruit. Using a square to represent the fruit, this model well described the mass and heat transfer during the drying process. The conduction process is considered to occur as a heat transfer inside the fruit, while the liquid diffusion is governed solely as mass transfer. The model included the constant diffusivity and thermal diffusivity as fixed properties. In this work, a mathematical model for heat and mass transfer during the drying process has been discretized using finite difference and implemented in MATLAB along with the initial and boundary conditions.

It was observed that the temperature is higher at the surface corner of the leading edge and lower at the symmetry leading edge. The depletion of water is more effective at the higher temperature of the surface, where the surface moisture is less than that at the surface corner. The fruit that is exposed to the surrounding air tends to warm up faster, causing the moisture content to decrease. The proposed model was able to provide information about moisture and temperature at all times, thus allowing detection of the region within the fruit, and a very important aspect in terms of food safety. The model allows us to predict temperature and moisture distribution as time increases.

Modelling of overall food behaviour is important and local and transient features can help to establish firmer knowledge for modelling applications. Simple processes allow researchers to base their development on a trial-and-error approach; more complex processes will quickly increase the required number of experiments. Moving from a trial-and-error approach to a quality by design approach requires the development of a model of the production process linking variables to critical quality attributes of the final product. Development of a user-friendly model for food drying can aid the development of a food product by shifting from a trial-and-error towards a quality-by-design approach.

References

- [1] Ceylan I 2009 Energy analysis of PID controlled heat pump dryer, *Engineering* **1** 188-195
- [2] Kaya A, Aydın O and Dincer I 2008 Experimental and numerical investigation of heat and mass transfer during drying of Hayward kiwi fruits (*Actinidia Deliciosa* Planch), *Journal of Food Engineering* **88** 323-330
- [3] Barati E and Esfahani J 2011 A new solution approach for simultaneous heat and mass transfer during convective drying of mango, *Journal of Food Engineering* **102** 302-309
- [4] Karim M A and Hawlader M 2005 Mathematical modelling and experimental investigation of tropical fruits drying, *International Journal of Heat and Mass Transfer* **48** 4914-4925
- [5] Shahari N, Jamil N, and Rasmani K A 2016 Comparative Study of Shrinkage and Non-Shrinkage Model of Food Drying, *Journal of Physics: Conference Series* **738** 012087
- [6] Tzempelikos D A, Mitrakos D, Vouros A P, Bardakas A V, Filios A E, and Margaritis D P 2015 Numerical modeling of heat and mass transfer during convective drying of cylindrical quince slices, *Journal of Food Engineering* **156** 10-21
- [7] Villa-Corrales L, Flores-Prieto J, Xamán-Villaseñor J and García-Hernández E 2010 Numerical and experimental analysis of heat and moisture transfer during drying of Ataulfo mango, *Journal of food engineering* **98** 198-206
- [8] Oztop H F and Akpınar E K 2008 Numerical and experimental analysis of moisture transfer for convective drying of some products, *International Communications in Heat and Mass*

Transfer **35** 169-177

- [9] Esfahani J, Majdi H and Barati E 2014 Analytical two-dimensional analysis of the transport phenomena occurring during convective drying: Apple slices, *Journal of Food Engineering* **123** 87-93
- [10] Shahari N, Rasmani K, and Jamil N 2016 Comparison between analytical and numerical solution of mathematical drying model, *AIP Conference Proceedings* **1705** 020043
- [11] Mohan V C and Talukdar P 2010 Three dimensional numerical modeling of simultaneous heat and moisture transfer in a moist object subjected to convective drying, *International Journal of Heat and Mass Transfer* **53** 4638-4650
- [12] Gulati T and Datta A K 2015 Mechanistic understanding of case-hardening and texture development during drying of food materials, *Journal of Food Engineering* **166** 119-138